Int. J. High Technology Ceramics **2** (1986) 33–45

Microstructure, Oxidation and Creep Behaviour of a β'-Sialon Ceramic

T. Chartier, J. L. Besson

Laboratoire des Matériaux Céramiques, LA CNRS 320, ENSCI,
87065 Limoges Cedex, France

and

P. Goursat

Laboratoire des Céramiques Nouvelles, LA CNRS 320, UER des Sciences,
87060 Limoges Cedex, France

SUMMARY

The ceramic material is fabricated by nitriding, followed by pressureless sintering, a mixture of silicon, aluminium and yttrium oxide powders (80·35:5·60:14·05 wt%). The samples, with 3% porosity, consist mainly of the solid solution β'-$Si_{6-z}Al_zO_zN_{8-z}$ *where* $z = 0{\cdot}4$, *with a small quantity of an yttrium silicate in an intergranular glassy phase. The main impurity elements are iron and calcium.*

The oxidation behaviour has been studied between 1150 and 1500°C. Weight gains are slow up to 1380°C and become rapid at higher temperatures. It is shown that the kinetics of the reaction are controlled by yttrium migration. Creep in 3-point bend tests has been examined in air. The deformation consists of viscoelastic and diffusional components. No cavitation has been observed.

The results are discussed in relation to the microstructure and its evolution during creep and oxidation experiments, and compared with current theories for silicon nitride-based ceramics.

1. INTRODUCTION

Due to the highly covalent Si–N bonding and the high temperature volatility of silicon nitride, the densification of silicon nitride requires the

Int. J. High Technology Ceramics 0267-3762/86/$03·50 © Elsevier Applied Science Publishers Ltd, England, 1986. Printed in Great Britain

use of sintering aids, usually metallic oxides, which by reacting with silicon dioxide present at the surface of the nitride grains, form eutectics that permit liquid-phase sintering. This liquid phase transforms during cooling into an intergranular nitrogen-containing glass, in which the impurities are segregated. The high temperature properties of the material are largely determined by the properties of the intergranular phase, that is, the nature and proportion of the sintering aids and impurities.

The material dealt with in this paper was processed by the Ceraver Company (France) as the starting point of a study that aims to define the minimum quantities of additives (aluminium and yttrium oxide) required to achieve high densification by pressureless sintering, together with good material properties.

2. MATERIAL

Silicon, aluminium and yttrium oxide powders (80·35 wt% Si + 5·60 wt% Al + 14·05 wt% Y_2O_3) are mixed in alcohol, dried and then nitrided between 1150 and 1400°C for 70 h. Table 1 shows the levels of chemical

TABLE 1
Impurity Levels and Grain Size Distribution of the Starting Powders

Powder	*Supplier*	*Purity*			*Granulometry* /μm		
		Ca	*Fe*	*Al*	d_{10}	d_{50}	d_{90}
Silicon	Baudier	<0·35 wt%[a] 0·02–0·14 wt%[b]	<0·6 wt%[a] 0·48–0·58 wt%[b]	≃0·5 wt%[a] 0·02–0·15 wt%[b]	0·35	0·82	1·35
Yttrium oxide	Rhone Poulenc	n.d.	50 ppm	n.d.	1·3	3·0	6·5
Aluminium	Seveau	43 ppm (CaO)	2 000 ppm (Fe_2O_3)		Specific surface area = 5·1 $m^2 g^{-1}$		

[a] Supplier's analysis.
[b] Ceraver analysis.

TABLE 2
Main Characteristics of the Nitrided and Milled Powder

Granulometry (μm)			*Specific surface area*	Si_3N_4 $\frac{\alpha}{\alpha+\beta} \times 100$
d_{10}	d_{50}	d_{90}		
0·23	0·87	1·9	3·04	81·3

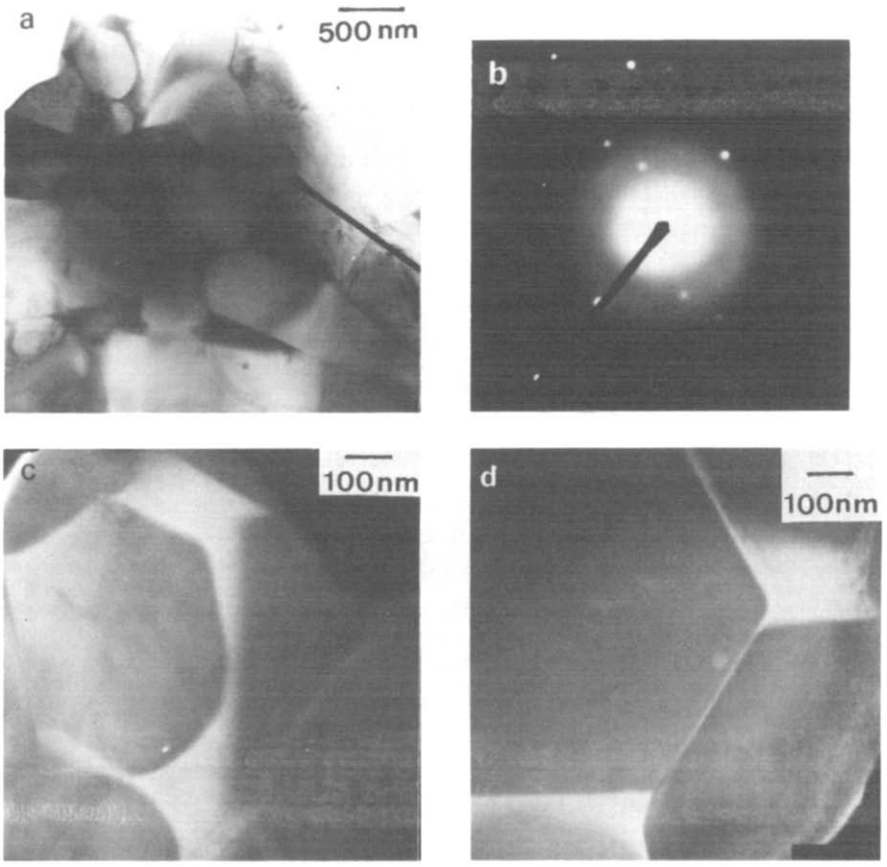

Fig. 1. TEM micrographs of the as-sintered material. (a) Bright field; example of microstructure of the as-sintered material. (b) Electron diffraction pattern of region (a) showing it is non-crystalline. (c) Associated dark field. (d) Another area showing amorphous pockets and glassy grain boundary phase between β'-sialon crystals.

impurities as provided by the manufacturers and determined by Ceraver. The main impurity elements are iron and calcium. After nitridation, the bricks (each weighing 15 kg) are attrition milled in white spirit. The main characteristics of the nitrided and milled powder are given in Table 2. The green samples are fabricated by injection moulding or isostatic pressing and pressureless sintered at 1700°C in a nitrogen atmosphere. The density is greater than 95% theoretical.

Microstructural observations show quite a large amount of glassy phase wetting the grains and forming rather big pockets in places (Fig. 1). The crystalline phases were identified by X-ray diffraction. The major phase is the β'-sialon solid solution. Minor quantities of the yttrium silicate, β-$Y_2Si_2O_7$, are also present. No yttrium aluminium garnet (YAG) was

detected. From the comparison of the a- and c-lattice parameters with those of pure Si_3N_4,[1,2] the composition of the β'-sialon solid solution was determined to be $Si_{5\cdot6}\ Al_{0\cdot4}\ O_{0\cdot4}\ N_{7\cdot6}$.

The test samples were cut using a wire-saw and acid leached with dilute hydrochloric acid to remove the iron contamination resulting from the cutting operation. The samples to be used for mechanical tests were carefully polished and the edges chamfered to reduce the possibility of edge flaws.

3. EXPERIMENTAL RESULTS

3.1. Oxidation

Oxidation behaviour in air was studied in the 1150–1500°C temperature range. Weight gains were detected only above 1300°C. The oxidation reaction is slow up to 1380°C and becomes fast at higher temperatures. The oxidation kinetics follow a parabolic law ($\alpha^2 = (\Delta m_t/\Delta m_\infty)^2 = Kt$, where Δm_t = weight gain at time t, Δm_∞ = weight gain for the complete reaction, and K = parabolic rate constant) throughout the test (24 h) at the lower temperatures. However, above 1380°C departures from the parabolic law are seen (Fig. 2). These departures occur sooner, the higher the temperature.

On polished cross-sections of samples, oxidized at 1200°C and above, a light-grey zone is noticed under the oxide scale (Fig. 3). The extent of this zone grows as the oxidation proceeds. This phenomenon, already

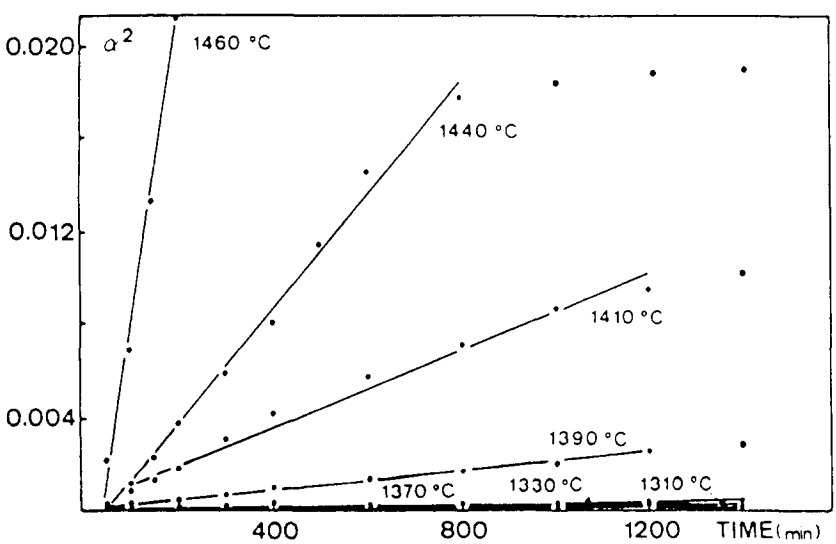

Fig. 2. Oxidation kinetics between 1310 and 1460°C in air.

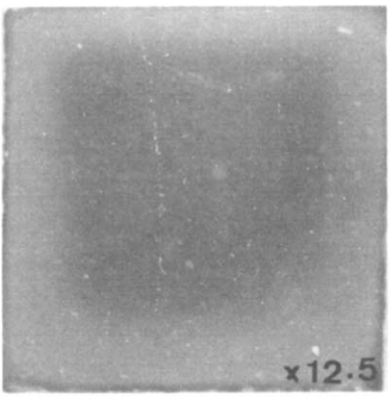

Fig. 3. Optical macrograph of a cross-section of a sample oxidized at 1300°C for 48 h. The lighter zone reveals the depth of oxygen penetration.

observed in the Si_3N_4–SiO_2–Y_2O_3 system,[3] corresponds to a selective oxidation of the intergranular phase. The oxide scale consists of acicular crystals in a glassy phase. The number and the size of the crystals increases with the oxidation temperature. The glassy phase is dense up to 1400°C and becomes gradually microporous and extremely friable after cooling (Fig. 4). The crystalline phases contained in the amorphous phase are cristobalite, a yttrium silicate (β-$Y_2Si_2O_7$ for $T < 1380$°C, δ-$Y_2Si_2O_7$ for $T > 1380$°C) and, in small quantity, for temperatures greater than 1400°C, yttrium aluminate $YAlO_3$. The proportion of yttrium silicate increases quickly with temperature.

Transmission electron microscopy (TEM) investigations of a sample oxidized at 1350°C for 48 h have revealed, in the bulk, microprecipitation resulting from partial devitrification of the intergranular glassy phase, but without a significant change in the total volume of the secondary phases (Fig. 5).

The concentration profiles of yttrium, calcium and aluminium were determined by X-ray microanalysis (EDAX) on a sample oxidized at 1260°C for 48 h (Fig. 6). Starting from the surface, three distinct zones are observed:

(i) a thin scale ($\sim 20\,\mu$m) corresponding to the oxide film in which the calcium and yttrium contents are high;
(ii) a zone depleted of yttrium and where the calcium content is no longer detectable;
(iii) a zone, 60–80 μm in width, where the yttrium concentration increases to reach the bulk concentration.

The entire thickness of these three zones is smaller than the light-grey

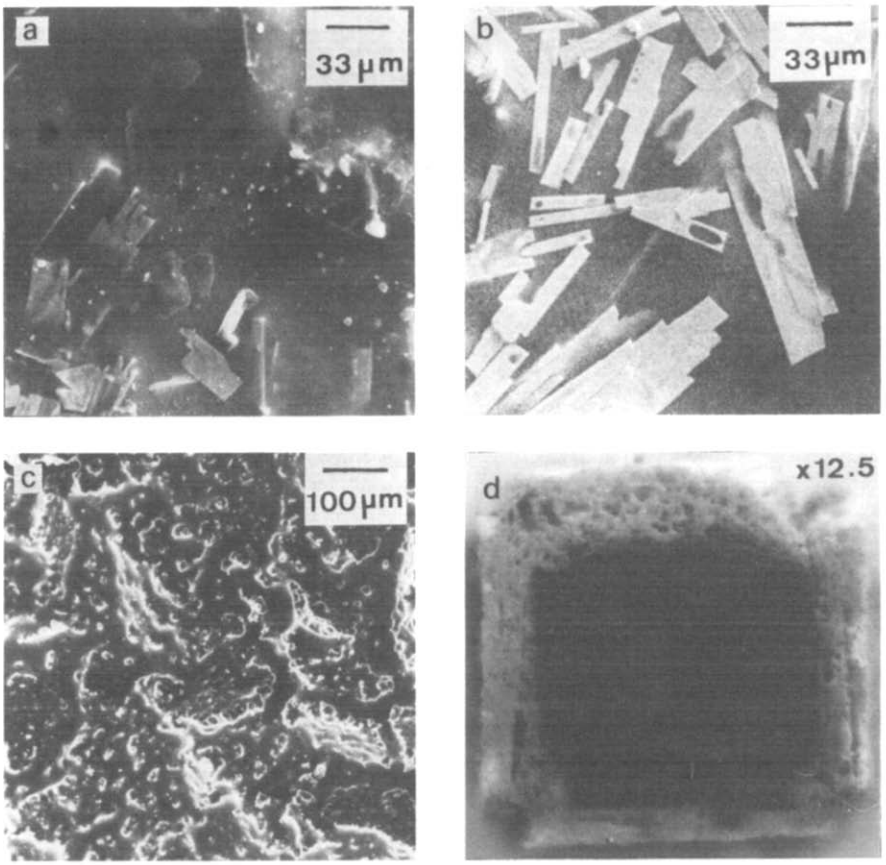

Fig. 4. SEM micrographs of surface of samples oxidized at (a) 1300°C, (b) 1400°C and (c) 1490°C; (d) cross-section of a sample oxidized at 1470°C.

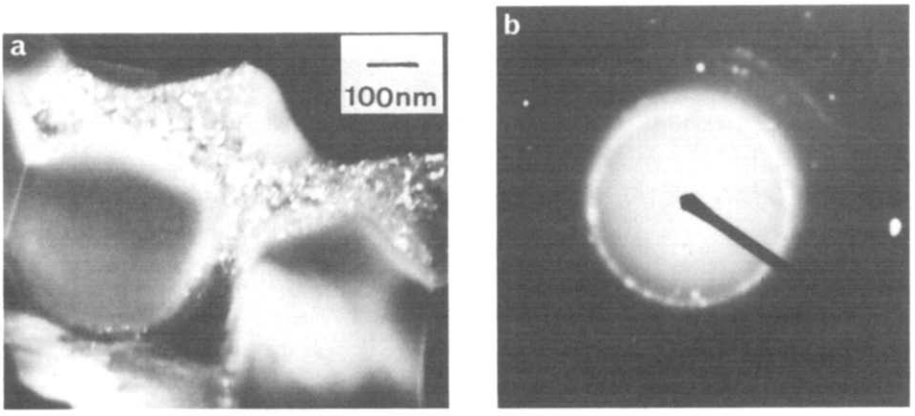

Fig. 5. (a) TEM micrograph of a sample after 48 h at 1350°C, showing microcrystallites in the glassy phase (dark field) (b) Associated electron diffraction pattern showing spotted rings.

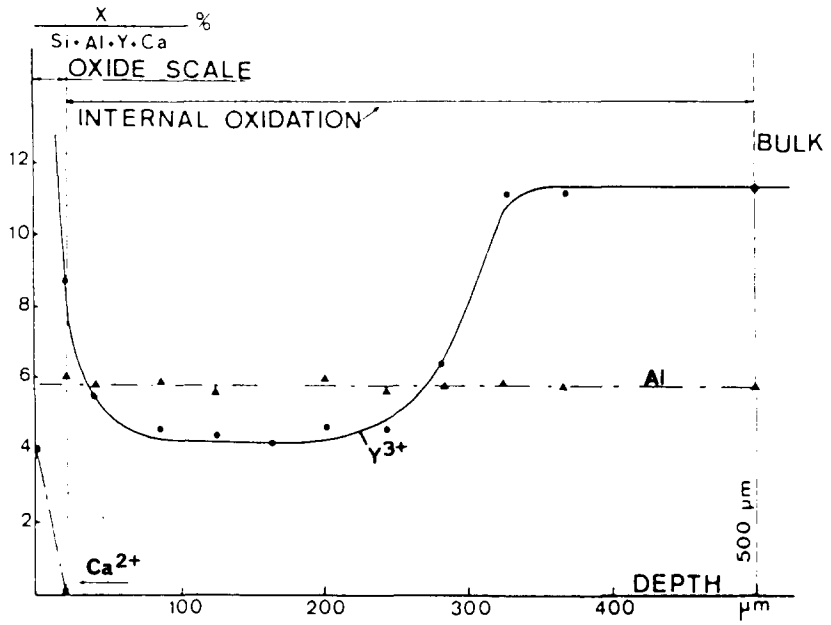

Fig. 6. Concentration profiles for yttrium, calcium and aluminium. Sample oxidized at 1260°C for 48 h.

zone which reflects the progress of the intergranular oxidation and the depth of oxygen penetration. Analyses carried out on the surface of samples oxidized respectively at 1200, 1260 and 1310°C show that the accumulation of yttrium in the oxide scale is already very high when weight gain begins to be detected by thermogravimetry (Table 3).

TABLE 3
Yttrium Concentration at the Surface After Oxidation for 48 h at Various Temperatures

	Bulk	*1 220°C*	*1 260°C*	*1 310°C*
$\frac{Y\%}{Si+Al+Y+Ca}$	12	15·7	26·8	43·3

It was noticed that the aluminium concentration remained uniform throughout the width of the samples and that iron concentrations never reached the detection threshold.

3.2. Creep

Creep in 3-point bend behaviour was investigated in air between 1100 and 1250°C, in the range 70–165 MPa. Below 1100°C, creep deformation was not measurable. A typical creep curve is presented in Fig. 7 ($T = 1150$°C,

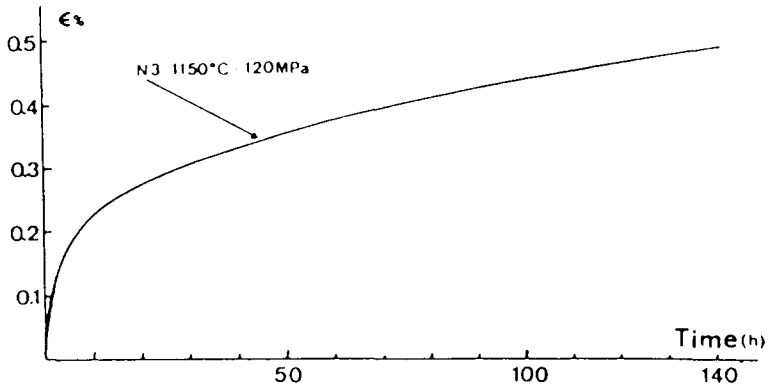

Fig. 7. Representative creep curve (1150°C, 120 MPa).

$\sigma = 120$ MPa). Following a rapid decrease over a few hours (corresponding to the primary stage) the creep rate diminishes very slowly. This stage will be referred to as the 'pseudo-steady-state' stage. Most of the creep tests were pursued until linear creep could be asserted. A true steady-state creep occurs only after a very long time (typically, times greater than 340 h). Tertiary creep was never observed under our experimental conditions. TEM observations of crept samples reveal a marked decrease in the quantity of the vitreous secondary phase. Neither cavitation nor micro-precipitates were observed (Fig. 8). The variation of Young's modulus versus temperature shows a rapid decrease above 1100°C that may be ascribed to the glass transition temperature of the amorphous intergranular phase. This is also the temperature at which the first signs of oxidation are observed.

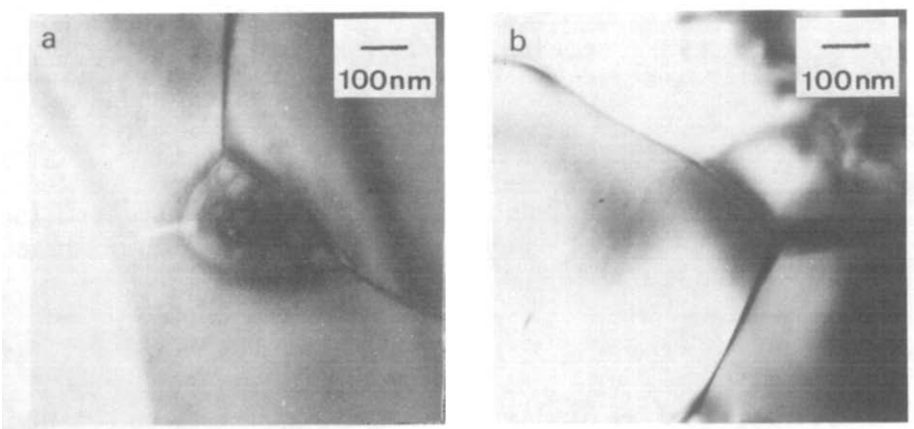

Fig. 8. TEM micrographs of crept samples illustrating the decrease in the amount of glassy phase (cf Fig. 1).

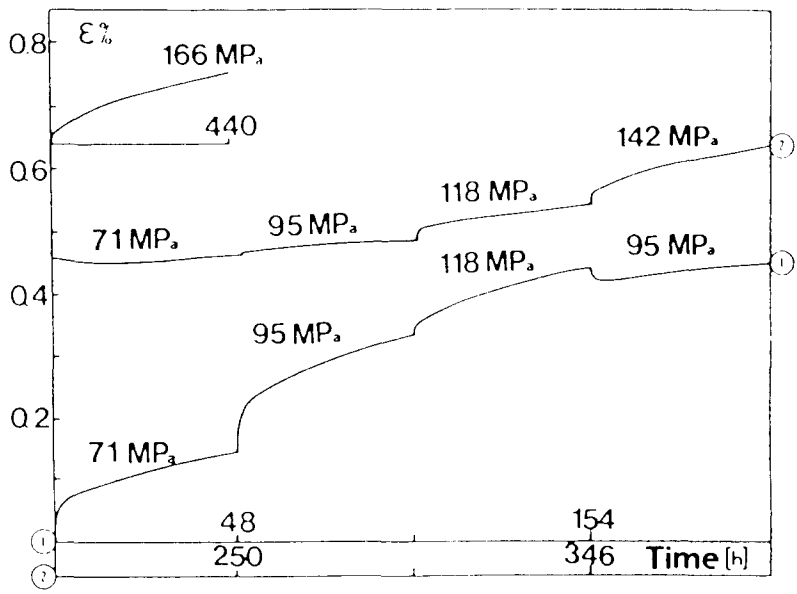

Fig. 9. Creep curve at 1150°C with increasing and decreasing stress increments. Notice negative creep rates for decreasing steps.

Usually, steady-state creep rates can be represented by the phenomenological relation:

$$\dot{\varepsilon} = A(S)\sigma^n \exp -\frac{E}{RT}$$

where σ = applied stress, n = stress exponent, E = apparent activation enthalpy, R = Boltzmann constant, T = absolute temperature and $A(S)$ = some function of the microstructure. If n and E are known identification of the mechanism that accounts for the deformation, and the activation enthalpy of the rate limiting step of the process may be possible. The study of n and E was carried out using, respectively, incremental stress changes at constant temperature and incremental temperature changes at constant stress. Each step lasted 48 h in both cases.

During the first stress steps (pseudo-steady-state stage) negative strain rates were observed when the stress was decreased (Fig. 9). On and after the seventh step (340 h), the creep rates vary linearly and reversibly with log stress. The slope of the line $\dot{\varepsilon}$ (log σ) is then equal to 1.

The growth of the creep rate with temperature also starts to be reversible from the seventh isothermal step (that is, after a creep time of about 340 h). Log $\dot{\varepsilon}$ versus T^{-1} then gives a straight line (Fig. 10). The apparent activation enthalpy was calculated to be $\simeq 780\,\mathrm{kJ\,mol^{-1}}$. An activation enthalpy of the same order of magnitude ($720\,\mathrm{kJ\,mol^{-1}}$) had

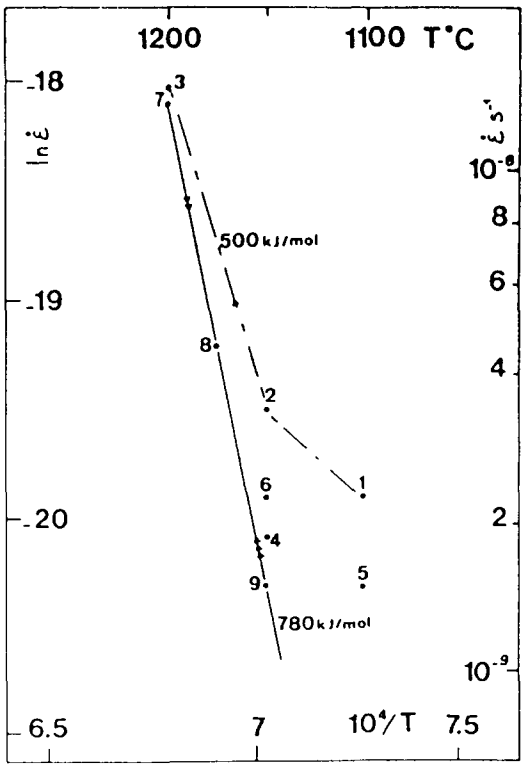

Fig. 10. Plot of $\ln \varepsilon$ versus reciprocal temperature for determination of the apparent activation energy for creep from incremental temperature tests.

been measured for creep in a silicon nitride type ceramic fabricated by hot-pressing from a mixture corresponding to 70 Si_3N_4–25 SiO_2–5 Y_2O_3 mol%.[3]

4. DISCUSSION

It is now well established that the high temperature behaviour of nitrogen ceramics is governed by the presence of secondary intergranular phases. In the present case oxidation and creep resistance begin to deteriorate at 1100°C, which is the glass transition temperature of the amorphous nitrogen-containing phase as indicated by the onset of the rapid decrease of the Young's modulus.

Oxidation starts with the formation of a superficial aluminosilicate film, formed by the reaction between oxygen and sialon which leads to a release of nitrogen, and continues with a selective attack of the intergranular vitreous phase which is more reactive than the grains. Oxygen migrates

inwards towards the bulk and nitrogen towards the outside. A gradient in chemical potential is created between the surface aluminosilicate and the intergranular phase. This induces a migration of the metal cations which react with the aluminosilicate and oxygen to form more complex silicates. This process is now well-established[4] but the details of the mechanism depend on the nature and concentration of the impurities and densification aids.

For the sialon under study, two temperature ranges may be distinguished: the first, from 1150 to about 1380°C, characterized by the formation of a compact and protective superficial oxide coating and a second, above 1380°C, where the oxide scale loses its protective efficiency. In the first range, the weight gain begins to be measurable at 1310°C. The parabolic form of the oxidation kinetics implies a diffusional mechanism. The absence of porosity in the oxide layer or separation at the grain boundaries suggests an ionic intergranular diffusion. From the data plotted in Fig. 2, the activation enthalpy for oxidation between 1300 and 1380°C was calculated to be $440 \pm 40\,\text{kJ mol}^{-1}$. The study of the inward shift to the light-grey front, associated with oxygen diffusion to the bulk, and of the concentration profiles of yttrium and calcium shows that the diffusion of the species commences at 1150°C and it seems likely that the limiting step is the same throughout the first temperature range. An activation enthalpy of $440\,\text{kJ mol}^{-1}$ is too high to be associated with oxygen diffusion for which the literature gives values of about $120\,\text{kJ mol}^{-1}$.[5,6] The alternative is then to assign this enthalpy to the migration of an 'yttrium–nitrogen' or 'calcium–nitrogen' compound species.

In the second range the higher temperature and the rapid accumulation of calcium at the surface lower the viscosity of the vitreous scale. The nitrogen released by the oxidation of the intergranular phase escapes more easily through the silica scale, creating a porosity that facilitates the access of oxygen to the internal interface (Fig. 4(d)). A diffusion regime is observed, for which the higher the temperature, the shorter the duration, and the determination of a rate constant becomes unreliable. In addition, after cooling, the oxide layer is very friable and it is no longer possible to determine concentration profiles for yttrium and calcium. The determination of the limiting step of the oxidation process is then purely speculative.

Concerning creep, Lange *et al.*[7] have proposed that the deformation of nitrogen ceramics is the sum of several components:

(i) a viscoelastic component, which is the main contribution to the strain during the primary stage and arises essentially from the response of the glassy intergranular phase;

(ii) a Coble diffusional component due to a mechanism of solution, migration in the glassy phase and precipitation which accommodates the stresses that arise at the ledges on grain boundaries during grain sliding; this component, characterized by a stress exponent equal to 1, is the major cause of deformation during steady-state creep;
(iii) under certain conditions, a cavitational creep.

The experimental features of creep behaviour of this material may be explained in the light of this theory. Thus, the negative creep rate, observed after a decreasing stress increment, is a consequence of the viscoelastic behaviour of the glassy phase.[8] The long pseudo-steady-state stage corresponds to the superposition of the viscoelastic and the diffusional components. The large decrease in glassy phase content observed in crept specimens explains the gradual decline of the viscoelastic contribution. When steady-state creep is established (for times above 350 h) the only remaining component is a diffusional one.

Because of the high viscosity of the yttrium-containing glassy phase[9] it is believed that the limiting step of the solution–migration–precipitation mechanism, acting during diffusional creep, is the same as for the sialon ceramic material studied in Ref. 3, as suggested by the similar values of activation enthalpy, that is, material transport through the intergranular phase.

Our conclusion is that material transport through the viscous glassy phase is rate-controlling for diffusional creep as well as for viscoelastic creep and oxidation. Hence, the main parameter is the viscosity of the glassy phase. The increase in the apparent activation enthalpy during creep must be related to that of the changes in chemical composition of the glassy phase with time. This view is supported by the fact that the slope of the curve $\ln \dot{\varepsilon}$ vs T^{-1} measured between the points 2 and 3 in Fig. 10 (that is, between 48 to 144 h of creep in air) leads to an 'activation enthalpy' of about 500 kJ mol^{-1}, which compares well with the value of 440 kJ mol^{-1} calculated for the oxidation process after 48 h exposure in air (that is, when a similar composition is reached for the glassy phase).

5. CONCLUSION

Oxidation in air of the β'-sialon material studied is slow up to 1380°C; for higher temperatures, the superficial oxide scale loses its protective efficiency and the oxidation becomes fast. In the lower temperature range the corrosion is intergranular and is accompanied by a migration of yttrium and calcium which accumulate in the oxide scale.

The creep deformation is the sum of a viscoelastic component and a

diffusional one, the relative proportions of which change with time and the characteristics of which are affected by modifications of chemical composition induced by oxidation and by the microstructural changes due to the applied stresses.

The rate-controlling step, for both oxidation and creep, has been ascribed to material transport through the intergranular phase. The activation enthalpy varies from 440 to 780 kJ mol^{-1} depending on the viscosity of the glassy phase which changes with its composition.

This study has allowed us to verify the possibility of fabricating pieces with good thermomechanical properties by injection moulding or isostatic pressing and pressureless sintering. It has established a standard for further studies of the improvements brought in by the choice of starting silicon powders with lower calcium impurity contents and the use of post-sintering thermal treatments.[10]

ACKNOWLEDGEMENTS

We wish to thank MM. L. Minjolle and W. Mustel for fabrication and machining of the samples as part of a collaborative research programme with Ceraver. We are also grateful to Dr P. Lortholary (Service de microscopie, Université de Limoges) for technical assistance. Financial support from the European Communities under contract SUT 111F was greatly appreciated.

REFERENCES

1. Jack, K. H., *J. Mater. Sci.*, **11** (1976) 1135.
2. Roult, G., Brossard, M., Labbe, J. C. and Goursat, P., Int. Conf. Non Oxide Tech. and Eng. Ceramics. Limerick, Ireland. 10–12 July 1985.
3. Bouarroudj, A., Goursat, P. and Besson, J. L., *J. Mater. Sci.*, **20** (1985) 1150.
4. Babini, G. N., Bellosi, A. and Vincenzini, P., *J. Mater. Sci.*, **19** (1984) 3487.
5. Deal, B. E. and Grove, A. S., *J. Appl. Phys.*, **36** (1965) 3770.
6. Tetard, D., Lortholary, P., Goursat, P. and Billy, M., *Rev. Int. Hautes tempér. Réfract.*, **10** (1973) 153.
7. Lange, F. F., Davis, B. I. and Clarke, D. R., *J. Mater. Sci.*, **15** (1980) 601, 611, 616.
8. Karunaratne, B. S. B. and Lewis, M. H., *J. Mater. Sci.*, **15** (1980) 449.
9. Babini, G. N., Bellosi, A. and Vincenzini, P., in *Science of Ceramics 11*, Eds R. Carlsson and S. Karlsson, Swedish Ceramic Society, 1981, 291.
10. Chartier, T., Besson, J. L., Goursat, P. and Mustel, W., in *Science of Ceramics 13*, 9–11 Sept. 1985, Orléans, France. To be published in *Journal de Physique-Colloques (Les Editions de Physique)*.

Received 25 April 1985; amended version received 25 September and accepted 30 September 1985.